TTC13 expression and STAT3 activation may form a positive feedback loop to promote ccRCC progression

Lingling Xie [Equal first author, 1], **Yu Fang** [Equal first author, 2], **Yangbo Guan** [Corresp., 3], **Jianping Chen** [1], **Wei Meng** [3], **Wenliang Gong** [Corresp. 2]

[1] Department of Laboratory Medicine, Affiliated Hospital of Nantong University, Nantong, China

[2] Department of Urology, Shanghai Changhai Hospital, Naval Medical University (Second Military Medical University), Shanghai, China

[3] Department of Urology, Affiliated Hospital of Nantong University, Nantong, China

Corresponding Authors: Yangbo Guan, Wenliang Gong
Email address: guanyangbo123@163.com, gongwl_uro@163.com

Background and Objectives: Renal cell carcinoma (RCC) originates from renal tubular epithelial cells and is mainly classified into three histological types, including clear cell renal cell carcinoma (ccRCC) which accounts for about 75% of all kidney cancers and is characterized by its strong invasiveness and poor prognosis. Hence, it is imperative to understand the mechanisms underlying the occurrence and progression of ccRCC to identify effective biomarkers for the early diagnosis and the prognosis prediction.

Materials and Methods: The mRNA level of TTC13 was quantified by RT-PCR, while the protein level was determined by western blot and immunohistochemistry (IHC) staining. Cell proliferation was measured by cck-8, and cell apoptosis was detected by flow cytometry. The binding of STAT3 to the promoter region of TTC13 was determined by the luciferase reporter assay and chip experiments. STAT3 nuclear translocation was assessed by immunofluorescence staining.

Results: We found that TTC13 was up-regulated in ccRCC, and TTC13 promoted cell proliferation as well as inhibited cell apoptosis and autophagy of ccRCC through wnt/β-catenin and IL6-JAK-STAT3 signaling pathways. Furthermore, TTC13 might play a role in the immune infiltration and immunotherapy of ccRCC. Mechanistically, STAT3 activated the transcription of TTC13 gene.

Conclusions: STAT3 directly regulated TTC13 expression through a positive feedback loop mechanism to promote ccRCC cell proliferation as well as reduce cell apoptosis and autophagy. These findings suggested new and effective therapeutic targets for more accurate and personalized treatment strategies.

Introduction

Renal cell carcinoma (RCC) ranks as the seventh most frequently diagnosed cancer and the second most common urinary system-related cancer worldwide. The incidence of RCC is different in different regions, as the developed countries show the highest incidence. RCC mainly includes three types, of which clear cell renal cell carcinoma (ccRCC) has the highest mortality rate [1]. ccRCC, characterized by hematuria, pain, and the lump in the kidney area, accounts for about 75% of all kidney cancers; nevertheless, ccRCC is often asymptomatic or insidious at the early stage. Although there is a significant improvement in the diagnosis and clinical treatment of ccRCC in recent years, the prognosis of patients with advanced ccRCC is still suboptimal due to the high risk of metastasis and poor response to radiotherapy and chemotherapy [2]. Therefore, understanding the underlying mechanisms of the neogenesis and the progression of ccRCC is critical to identify potential biomarkers for early diagnosis, treatment selection, and prognosis prediction.

Tetratricopeptide repeat domain 13 (TTC13), expressed in 27 tissues including the brain, bladder, heart, and lung, is a member of a large family of proteins named tetratricopeptide repeats (TPR), which structurally consists of a degenerate, 34 amino acid repeats. TPR-containing proteins are found not only in many organisms but also in various subcellular locations, including cytoplasm, nucleus, and mitochondria. Functionally, the TPR domain plays a role in chaperone, cell cycle, transcription, and protein transport [3]. Although the role of TPR-related proteins in tumors has been reported in leukemia, liver cancer, and gastric cancer [4, 5], the function of TTC13 in tumors is not clear, and the expression and the biological functions of TTC13 in ccRCC remain to be determined.

In this study, we performed multiple bioinformatics analyses and validation experiments to explore the expression, biological functions, and prognostic value of TTC13 in ccRCC. We for the first time found that TTC13 was up-regulated in ccRCC, and TTC13 expression was associated with several pathological features and signaling pathways. In particular, TTC13 could potentially be involved in modulating immune infiltration and immunotherapy. Our findings suggest that TTC13 may serve as a valuable independent prognostic biomarker for ccRCC. Our mechanistic studies indicated that TTC13 might contribute to ccRCC progression via Wnt/β-catenin and IL6-JAK-STAT3 signaling pathways. Taken together, TTC13 may play a significant role in ccRCC occurrence and progression, and TTC13 signaling axis my serve as novel and effective therapeutic targets

for the development of more accurate and personalized treatment strategies.

Materials and methods

Bioinformatics analysis

The single gene expression data for TTC13, as well as its corresponding clinical data, were obtained from The Cancer Genome Atlas (TCGA) database. The raw data underwent pre-processing using either log2 transformation or normalization and then were analyzed using R software. Differential gene expression of TTC13 was calculated using the "limma" R package, with a cut-off criterium of |log2 fold change (FC)| > 1 and a false discovery rate (FDR) < 0.05. The flow chart of this article was shown in Figure 1.

Human ccRCC tissue samples and cell lines

The tumor and adjacent non-cancerous tissues were obtained from Affiliated Hospital of Nantong University. The study was approved by the hospital's ethics committee(Institutional Review Board approval number: 2022-K003-02), and all patients provided written informed consent for the use of their tissue samples. Normal HK-2 cell line and three ccRCC cell lines: A498, 786-O, and Caki-1, were obtained from either the Cell Bank of Chinese Academy of Sciences (Shanghai, China) or Procell Life Science & Technology Co. Ltd. (Wuhan, China). All cell lines were maintained according to the required culture conditions.

Antibodies

The following antibodies were used in this study: TTC13 (LSBio, USA), Bax, Bcl-2, IL-6, cleaved-caspase-3, LC3 Ⅱ / Ⅰ, P62, JAK2, Ki67, MMP9, phosphor-JAK2, phosphor-STAT3, STAT3, β-catenin, GAPDH and β-actin (Cell Signal Technology, MA, USA).

Quantitative Real-Time Polymerase Chain Reaction (qRT-PCR)

qRT-PCR was performed to examine the expression level of TTC13 in 64 paired ccRCC tumor and adjacent non-cancerous samples according to the manufacturer's instructions using ABI 7500. Duplicate real-time PCR analyses were performed for each sample, and the obtained threshold cycle (CT) values were averaged. TTC13 gene expression was normalized to the expression of housekeeping gene (GAPDH) resulting in the ΔCT value, where ΔCt = Ct Target − Ct GAPDH. The relative expression level was calculated by $2^{-\Delta CT}$ as previously described[6].The primers were synthesized by Tsingke Biotech (Shanghai, China), and the primer sequences were as follows: for TTC13, forward 5′-GACTCAGACTGCGAACCCAA-3′ and reverse 5′-

ACTTGGCCTGGCTCAGAATC-3′; for GAPDH, forward 5′-GAGTCAACGGATTTGGTCGT-3′ and reverse 5′-GACAAGCTTCCCGTTCTCAG-3′.

Cell transfection

shRNA for TTC13 gene silencing and the plasmid for TTC13 overexpression were purchased from GenePharma (Shanghai, China). The shRNA1 sequence was: 5′- GCAGTGAATGACCTCACTAAA-3′, the shRNA2 sequence was: 5′-GCTTACAGGAAGCCCTTAAGA-3′. The TTC13 shRNA or overexpression plasmid was transiently transfected into ccRCC cells using Lipofectamine 3000, and the transfection efficiency was confirmed by western blot analysis. Cells were collected for in vitro and in vivo functional experiments 48 h after transfection.

Cell proliferation and apoptosis

Cell proliferation was determined by a CCK-8 detection kit (Beyotime, Haimen, China). Briefly, transfected cells were seeded into 96-well plate (5,000/well) and cultured for the indicated time. CCK-8 solution (10 μl) was added to each well at specific time points, and the absorbance at 450 nm was measured by a plate reader. Each experiment was independently repeated five times. For apoptosis assay, the ccRCC cells were collected, stained with annexin V-conjugated fluorescein isothiocyanate (FITC) and propidium iodide (PI) (BD Biosciences, Franklin Lakes, NJ, USA) according to the manufacturer's protocol, and analyzed using FACScanTM flow cytometer (BD Biosciences).

Mouse tumor xenografts

Six-week-old male null mice (weighted about 18g) were obtained from Jihui Laboratory Animal Care Co., Ltd. (Shanghai, China) and were randomly divided into two groups for subcutaneous injection with 786-O cells (1×10^7/ml, 200 μl) either expressing NC plasmid or TTC13 shRNA expressing plasmid. The xenograft tumor growth was monitored every 5 days, and at day 35, the tumors were dissected, weighed, and subjected to immunohistochemistry (IHC) staining. All experimental procedures were performed in accordance with the institutional guidelines approved by the Shanghai Changhai Hospital, Naval Medical University.

Western blot analysis

Total proteins were extracted from ccRCC cells using the protein extraction kit (Beyotime, Haimen, China) and quantified by the NanoPhotometer (Implen, Inc., CA, USA). Then, the proteins were separated by SDS-

PAGE and transferred onto PVDF membranes, followed by incubation with primary antibodies. After extensive washing, the PVDF membranes were incubated with corresponding secondary antibodies, and the specific protein bands were visualized using an enhanced chemiluminescence (ECL) kit (Beyotime, Haimen, China) and imaged in a gel imaging system.

Immunohistochemistry (IHC) staining

The protein expression and distribution of β-catenin, Ki67, MMP9, phospho-STAT3, and TTC13 were examined by IHC using Paraffin-embedded sections of ccRCC and adjacent non-cancerous tissues. Briefly, after deparaffinization and rehydration, the paraffin slides were placed in citric acid buffer solution (pH=6.0), heated at 121 °C for 15 minutes in an autoclave, and treated with 3% hydrogen peroxide for 20 min. Slides were blocked with 1% BSA for 15 minutes and then incubated with primary antibody (1:50 dilution) at 4 °C overnight. After extensive washing, the slides were incubated with goat anti-rabbit IgG-HRP secondary antibody (1:100 dilution) at room temperature for 1 h and then counterstained with hematoxylin for 30 s. Lastly, the conventional dehydration was performed, and the slides were examined as well as imaged under a microscope (DM500, Leica).

Immunofluorescence staining

The ccRCC cells were pretreated, seeded onto coated coverslips, fixed with paraformaldehyde, permeabilized, and then incubated with primary antibodies overnight at 4 °C followed by incubation with secondary antibodies for 1 h. The cells were subsequently stained with 0.1 μg/ml DAPI for 1 minute at room temperature in the dark. The coverslips were mounted, and the images were acquired using a fluorescence microscope.

Luciferase reporter assay and Chromatin immunoprecipitation (ChIP) assay

Caki-1 cells treated with AG490 were transiently co-transfected with pGL3-basic-TTC13 promoter reporter plasmid and pRL-TK expression construct using Lipofectamine 3000 reagent following the manufacturer's instructions. At 48 h after transfection, the cells were harvested, and the luciferase activity was quantified using the Bright-Glo™ Luciferase assay kit (Promega Corporation), which was normalized to the Renilla luciferase activity. Each experiment was performed in triplicate. For the chip assay, a standard chip protocol was used for ccRCC cells crosslinking, nuclear isolation, and chromatin fragmentation. The fragmented chromatin was

incubated with anti-STAT3 antibody at 4°C overnight, and the eluted chromatin was subjected to quantitative PCR analysis. IgG was used as a negative control.

Statistical analysis

Statistical analyses were conducted using GraphPad Prism 8.0 and SPSS Statistics 22.0. Data were presented as median and standard error of the mean (SEM). To compare the overall survival between the two groups, Kaplan-Meier (K-M) curves and the log-rank test were employed. Paired cases were analyzed using t-test, while the prognostic value of TTC13 was evaluated using univariate and multivariate Cox regression analyses. A P-value <0.05 was considered statistically significant, and significance levels were denoted as follows: *P<0.05, **P<0.01, ***P<0.001.

Results

TTC13 was upregulated in ccRCC

As shown in Figure 2A, the expression level of TTC13 was different between various tumors and normal tissues, and the expression level of TTC13 was significantly higher in ccRCC tissues than in normal tissues (Figure 2B) ($P < 0.001$), which was supported by the data from the paired tumor and non-cancerous samples (Figure 2C). Consistently, qRT-PCR analysis (tumor = 64, normal = 64) showed that the mRNA level of TTC13 was significantly higher in ccRCC tissues than in normal tissues (P =0.0018) (Figure 2D) which was further confirmed by western blotting (Figure 2E, G) and IHC (Figure 2F). Meanwhile, the ROC curves were used to evaluate the diagnostic efficacy of TTC13 expression for ccRCC, and the area under the curve (AUC) for the 1-, 3-, and 5-year survival was 0.751, 0.799 and 0.779, respectively (Figure 2H). Moreover, the ccRCC patients were divided into low- and high-expression groups based on the median value of TTC13, and the K–M survival curve analysis showed that the overall survival of the high-expression group was worse than that in the low-expression group ($P < 0.001$) (Figure 2I).

TTC13 promoted the proliferation and inhibited the apoptosis and autophagy of ccRCC cells

We next explored the biological functions of TTC13 in ccRCC. CCK-8 assay showed that knockdown of TTC13 inhibited the proliferation of 786-O and Caki-1 cells (Figure 3A, B). On the other hand, the flow cytometry analysis revealed that knockdown of TTC13 increased the apoptosis of ccRCC cells (Figure 3C). In support with these findings, western blotting results indicated that the levels of p62 and BCL-2 protein in

shTTC13 transfected 786-O and CAKi-1 cells were significantly decreased, while the levels of Bax and cleaved caspase-3 as well as the ratio of LC3-II/I were significantly increased. Conversely, TTC13 overexpression resulted in the opposite effects (Figure 3D, E), suggesting that TTC13 was involved in the regulation of renal cancer cell survival and autophagy.

TTC13 silencing inhibited tumor growth in vivo

To explore whether TTC13 affected ccRCC tumor growth in vivo, we subcutaneously injected 786-O cells transfected with TTC13 NC or shRNA plasmid into nude mice and found that the tumor volume and weight of the shRNA group were significantly smaller than that of the NC group (Figure 4A, B, C, D). Furthermore, IHC staining showed that the expression of TTC13, proliferation marker Ki67, metastasis marker MMP9, β-catenin, and p-STAT3 were lower in the shRNA group than in the NC group (Figure 4E). Together, these results indicated that knockdown of TTC13 effectively inhibited tumor growth in vivo.

TTC13-related signaling pathways in ccRCC

The TTC13-related signaling pathways were discovered by GSVA analysis to elucidate the role of TTC13 in the pathogenesis of ccRCC. The GSVA analysis was carried out in the high and low TTC13 expression datasets. We identified TTC13 associated up- and down-regulated signaling pathways, including wnt/β-catenin, IL6-JAK-STAT3, PI3K-Akt-MTOR, bile acid metabolism, and estrogen-response-late signaling pathways (Figure 5A). To validate the findings from bioinformatics analysis, we experimentally determined whether wnt/β-catenin and IL6-JAK-STAT3 signaling pathways were activated in ccRCC by examining the expression of TTC13, β-catenin, STAT3, p-STAT3, JAK2, p-JAK2 in ccRCC tumor tissues and adjacent normal tissues. Western blotting results demonstrated activated wnt/β-catenin and IL6-JAK-STAT3 signaling pathways in ccRCC (Figure 5B, C). To directly demonstrate the relationship between TTC13 and wnt/β-catenin and IL6-JAK-STAT3 signaling pathways, we assessed the effects of TTC13 overexpression or knockdown on them. We found that overexpression of TTC13 enhanced, while TTC13 knockdown inhibited, the expression of p-JAK-2, p-STAT3, β-catenin in ccRCC cells (Figure 5D).

TTC13 contributed to ccRCC progression via wnt/β-catenin and IL6-JAK-STAT3 signaling pathway

Having demonstrated that TTC13 activated wnt/β-catenin and IL6-JAK-STAT3 signaling pathways in ccRCC, we speculated that TTC13 might contribute to ccRCC progression through the above two signaling

pathways. To test this hypothesis, we performed rescued experiments using a specific inhibitor of wnt/β-catenin or IL6-JAK-STAT3 signaling pathway and found that the inhibitor could attenuate the growth-promoting effect of TTC13 individually, with synergistic effect when used in combination in CCK-8 and apoptosis assay (Figure 6A, B, C). Western blot analysis showed the similar results (Figure 6D, E).

STAT3 activated the transcription of TTC13 gene

More importantly, we investigated the molecular mechanisms underlying the elevated TTC13 expression in ccRCC. Since we observed that TTC13 could activate the IL6-JAK-STAT3 signaling pathway, we speculated that STAT3 should enter the nucleus upon TTC13 activation. Indeed, immunofluorescence staining confirmed a significant translocation of STAT3 from cytoplasm to nucleus when TTC13 was overexpressed (Figure 7E). Because STAT3 is a transcription factor, we next explored whether STAT3 affected the activity of the TTC13 promoter. There were potential STAT3 binding sites on TTC13 promoter region identified by the transcription factor binding profile database JASPAR (http://jaspar.genereg.net/) (Figure 7A, B). We then performed the luciferase reporter assay and found that the relative luciferase activity in AG490-treated Caki-1 cells were significantly reduced (Figure 7D). Chip experiments further confirmed that STAT3 directly bound to the TTC13 promoter (Figure 7C), suggesting that STAT3 might directly regulated TTC13 expression through a positive feedback loop mechanism to promote ccRCC cell proliferation, as well as to reduce cell apoptosis and autophagy.

Discussion

RCC is the seventh most common cancer and the second most common cancer in the urinary system worldwide, with an increasing rate of 2% every year. RCC is a tumor of renal tubular epithelial cell origin and mainly contains three histological types: ccRCC, chromophobe RCC, and papillary RCC. ccRCC is the most common histological subtype, accounting for more than 75% of all diagnosed kidney tumors, and has the characteristics of strong invasiveness and poor prognosis [7, 8]. Due to insufficient understanding of the pathogenic mechanisms of ccRCC, it is difficult to diagnose at the early stage and predict the prognosis of ccRCC patients; hence, effective treatment strategies to prolong the survival of patients with advanced ccRCC are still under development. Therefore, there is an urgent need to identify new and effective biomarkers for the early diagnose and the prognosis prediction of ccRCC patients. In line with this, the exploration of the mechanisms related to ccRCC is also particularly important.

Tetratricopeptide repeat domain 13 (TTC13) is a member of a large family of proteins named tetratricopeptide repeats (TPR), which contains more than 5,000 members. TTC13 mRNA was ubiquitously expressed in all mouse tissues; however, TTC13 protein expression varies in different tissues with a high expression in both the kidney and the liver. So far, to the best of our knowledge, there is no reported study on the expression and potential functions of TTC13 in ccRCC. In our study, we analyzed the expression level and the prognostic value of TTC13 in ccRCC as well as explored the its biological functions via both the bioinformatics analysis and the experimental confirmation. Our experimental results showed an upregulation of TTC13 at both mRNA and protein levels in ccRCC cells as well as in ccRCC tissues. In addition, ccRCC patients with high TTC13 expression had poor prognosis. Furthermore, overexpression of TTC13 promoted the proliferation of ccRCC cells, while inhibited the apoptosis and autophagy of cells. Hence, our results suggested that TTC13 might play a key role in the occurrence and progression of ccRCC (Figure 8). Moreover, the univariate and multivariate Cox regression analyses confirmed that TTC13 was an independent predictor for ccRCC. Notablely, we constructed a nomogram including TTC13 to assist clinicians accurately predict the prognosis of ccRCC patients.

The Wnt/β-catenin signaling pathway is a conserved signaling cascade involved in a variety of physiological processes, such as proliferation, differentiation, apoptosis, migration, invasion, and tissue homeostasis. Accumulating evidence has revealed that the dysregulation of the Wnt/β-catenin signaling pathway contributes to the development and progression of several solid tumors and hematological malignancies [9-12]. In this study, we discovered that the Wnt/β-catenin signaling pathway was also abnormally expressed in ccRCC, suggesting the involvement of Wnt/β-catenin in ccRCC. In addition, IL6-JAK-STAT3 pathway is abnormally overactivated in many cancer types, which is often associated with poor outcomes [13, 14]. It is known that the IL6-JAK-STAT3 pathway has a huge impact on various biological progressions of tumors, such as migration, invasion, and angiogenesis [15]. Moreover, the activation of this pathway is also associated with suppressed antitumor immune responses in the tumor microenvironment. Therefore, therapies targeting this pathway may benefit cancer patients by simultaneously inhibiting tumor cell growth and stimulating anti-tumor immunity. Thus, targeting the IL6-JAK-STAT3 pathway is a promising therapeutic modality. Indeed, many new IL-6/JAK/STAT3 pathway inhibitors have been developed, some of which are in preclinical and/or clinical

evaluation. Nevertheless, few studies have reported the IL6-JAK-STAT3 pathway signature in ccRCC. In this study, we found that the IL6-JAK-STAT3 signaling pathway was activated in ccRCC, suggesting the therapeutic significance of this pathway. In support with our findings, Zhan et al also identified the IL6-JAK-STAT3 pathway as a potential risk factor in ccRCC by univariate and multivariate Cox regression analysis [14].

Our subsequent study demonstrated that overexpression of TTC13 could activate the IL6-JAK-STAT3 and Wnt/β-catenin signaling pathways, whereas knockdown of TTC13 suppressed the two signaling pathways. Further experiments indicated that TTC13 promoted ccRCC cell proliferation and restrained apoptosis or autophagy through IL6-JAK-STAT3 and Wnt/β-catenin signaling pathways. Similar to our findings, Wang et al [16] has reported that CENPA promoted the progression of ccRCC by activating the Wnt/β-catenin signaling pathway. Knockdown of CENPA significantly down-regulated while overexpression of CENPA up-regulated the expression of β-catenin and its target gene cyclin D1 in ccRCC. Importantly, overexpression of CENPA facilitated, while knockdown of CENPA reduced the translocation of β-catenin into the nucleus. In addition, a recent study has revealed the Wnt/β-catenin pathway-induced ARL4C expression in ccRCC [17]. On the other hand, several studies have shown that some genes act as tumor suppressors by inhibiting the Wnt/β-catenin signaling pathway in ccRCC. For example, Gorka et al [18] has reported that compared with the negative control, β-catenin in ccRCC cells is significantly reduced at both mRNA and protein levels by MCPIP1 overexpression, and the levels of both active forms of β-catenin were reduced. Interestingly, immunofluorescence staining showed that loss of MCPIP1 RNase activity resulted in the translocation of β-catenin into the nucleus. In consistent to this, silencing MCPIP1 in ccRCC cells increased the expression levels of active β-catenin and the transcriptionally active form of β-catenin. Therefore, the level of β-catenin was negatively correlated with the level of MCPIP1. In line with these findings, Xu et al. [19] reported that the upregulation of SDHA resulted in a significant suppression of the Wnt/β-catenin signaling pathway by decreasing the protein expression of p-GSK-3β, β-catenin, and c-Myc in ccRCC cells. However, these effects were notably mitigated upon activation of the Wnt/β-catenin signaling pathway. Phenotypically, SDHA impairs cell viability and inhibits proliferation, migration and invasion of ccRCC cells. Moreover, overexpression of TLN2 significantly suppressed the expression of activated β-catenin, cyclin D1 and c-Myc in ccRCC cells. Activator of Wnt/β-catenin signaling pathway can attenuate the inhibition on the malignancy of ccRCC cells caused by TLN2 overexpression [20].

And SOX17 displayed the similar function as TLN2 [21]. These results, together with our findings, provided supporting evidence that Wnt/β-catenin signaling pathway is a crucial regulator in the progression of ccRCC, highlighting the clinical therapeutic significance of targeting this signaling pathway.

As for IL6-JAK-STAT3 signaling pathway, consistent with our findings, Wang et al [22] also reported that the expressions of G3BP1, IL-6 and p-STAT3 in renal cell carcinoma tissues were significantly higher compared with adjacent normal tissues. Knockdown of G3BP1 significantly inhibited the phosphorylation of STAT3 in RCC cells. Furthermore, the expression of G3BP1 in RCC tissues was positively correlated with IL-6 and p-STAT3 level, suggesting that IL-6, G3BP1 and STAT3 are correlated with each other in primary renal cell carcinoma. Another study found that knockdown of circ_0000274 RNA expression significantly reduced the protein levels of p-JAK1/JAK1 and p-STAT3/STAT3 in 786-O and A498 cells, while inhibiting miR-338-3p expression reversed this effect [23]. In addition, the conditioned medium of TAMs increased the phosphorylation level of STAT3 in RCC cells [24]. Furthermore, tumor-associated macrophages promoted RCC invasion, migration and epithelial-mesenchymal transition by activating IL-6/STAT3 signaling. Consistent with these findings, another study showed that the total pSTAT3 and nuclear pSTAT3 levels were significantly increased in ccRCC tissues compared with the adjacent tissues. The level of pSTAT3 and the number of pSTAT3+ nuclei were significantly increased in ccRCC patients with low serum Vitamin D. More importantly, active vitamin D3 effectively inhibited LPS-induced STAT3 phosphorylation in ccRCC cells, suggesting the clinical value of vitamin D in ccRCC [25]. Chae et al [26] also reported that Thymoquinone inhibited the phosphorylation of JAK2/STAT3 in ccRCC and the subsequent expression of downstream target genes involved in cell proliferation and anti-apoptosis, such as cyclin D1, cyclin D2, and survivin. In addition, Thymoquinone effectively prevented the phosphorylated from of STAT3 from entering the nucleus and binding to DNA to activate the transcription of target genes. Further studies revealed that Thymoquinone induced apoptosis in ccRCC cells through reactive oxygen species-mediated inactivation of the JAK2/STAT3 pathway. Similarly, SIRT1 destabilized STAT3 through the ubiquitin-proteasome pathway, resulting in decreased STAT3-dependent FGB expression, which in turn inhibited RCC cell proliferation [27].

One important finding of our study was that STAT3 bound to the promoter of TTC13 gene to upregulate the expression of TTC13, which in turn further activated the JAK2/STAT3 signaling pathway to increase the

nuclear import of STAT3, thereby forming a positive feedback loop to promote the progression of ccRCC. A recent investigation had also revealed that the JAK/STAT3 signaling pathway mediated RCC cell apoptosis and glycolysis by RNF7, as STAT3 directly binded to RNF7 promoter [28]. Taken together, these data suggested that IL6-JAK-STAT3 signaling pathway played a key role in the pathogenesis of ccRCC, providing the rationale of targeting this pathway in ccRCC treatment.

Nonetheless, this study also had some limitations. First, we used retrospective data from public databases, which needed validation in larger cohorts of ccRCC patients with well-defined clinical staging and sufficient clinical data. In addition, the biological functions of TTC13 in ccRCC need to be further explored. Lastly, it is necessary to improve and standardize the detection method of TTC13 gene to increase the feasibility of clinical application.

Conclusions

In conclusion, we were the first to use a variety of bioinformatics methods and verification experiments to explore the expression and clinical value of TTC13 in ccRCC. Our results suggested that TTC13 might play a role in the proliferation, apoptosis and autophagy of ccRCC. In addition, TTC13 might serve as a new biomarker for the diagnosis and prognosis prediction for patients with ccRCC.

Funding This study was funded by Nantong Commission of Health (QN2022016).

Compliance with Ethical StandardsEthics statements

The study was approved and consented by the Ethics Committee of the Affiliated Hospital of Nantong University(2022-K003-02) and Naval Medical University, SYXK (Shanghai) 2022-0011. All patients provided written informed consent for the use of their tissue samples.

Conflict of Interest The authors declare that there is no conflict of interest.

Acknowledgments

We sincerely thank The Cancer Genome Atlas (TCGA) database for providing and managing patient data. The authors express their appreciation for the assistance by Shanghai Changhai Hospital, Naval Medical University, which was instrumental in facilitating this research. Flow chart section drawing material from Figdraw (Fig. www.figdraw.com), this material ID: UOAUR7ce55.

298

299 **References**

300

301 1. Piao, X.M., et al., *A New Treatment Landscape for RCC: Association of the Human Microbiome with*
302 *Improved Outcomes in RCC.* Cancers (Basel), 2023. **15**(3).
303 2. Kase, A.M., D.J. George, and S. Ramalingam, *Clear Cell Renal Cell Carcinoma: From Biology to*
304 *Treatment.* Cancers (Basel), 2023. **15**(3).
305 3. Leontiou, I., et al., *The Bub1-TPR Domain Interacts Directly with Mad3 to Generate Robust Spindle*
306 *Checkpoint Arrest.* Curr Biol, 2019. **29**(14): p. 2407-2414 e7.
307 4. Shaheen, R., et al., *Biallelic Mutations in Tetratricopeptide Repeat Domain 26 (Intraflagellar Transport*
308 *56) Cause Severe Biliary Ciliopathy in Humans.* Hepatology, 2020. **71**(6): p. 2067-2079.
309 5. El-Daher, M.T., et al., *Tetratricopeptide repeat domain 7A is a nuclear factor that modulates*
310 *transcription and chromatin structure.* Cell Discov, 2018. **4**: p. 61.
311 6. Aguilar-Briseno, J.A., et al., *TLR2 on blood monocytes senses dengue virus infection and its expression*
312 *correlates with disease pathogenesis.* Nat Commun, 2020. **11**(1): p. 3177.
313 7. Ye, S., et al., *GBP2 promotes clear cell renal cell carcinoma progression through immune infiltration*
314 *and regulation of PD-L1 expression via STAT1 signaling.* Oncol Rep, 2023. **49**(3).
315 8. Narisawa, T., et al., *Fibroblast growth factor receptor type 4 as a potential therapeutic target in clear*
316 *cell renal cell carcinoma.* BMC Cancer, 2023. **23**(1): p. 170.
317 9. Di Bartolomeo, L., et al., *Wnt Signaling Pathways: From Inflammation to Non-Melanoma Skin Cancers.*
318 Int J Mol Sci, 2023. **24**(2).
319 10. Muto, S., et al., *Wnt/beta-Catenin Signaling and Resistance to Immune Checkpoint Inhibitors: From*
320 *Non-Small-Cell Lung Cancer to Other Cancers.* Biomedicines, 2023. **11**(1).
321 11. Han, S., et al., *LAPTM5 regulated by FOXP3 promotes the malignant phenotypes of breast cancer*
322 *through activating the Wnt/beta-catenin pathway.* Oncol Rep, 2023. **49**(3).
323 12. Li, R., et al., *G6PD promotes cell proliferation and dexamethasone resistance in multiple myeloma via*
324 *increasing anti-oxidant production and activating Wnt/beta-catenin pathway.* Exp Hematol Oncol,
325 2022. **11**(1): p. 77.
326 13. Ni, J.S., et al., *miR-515-5p suppresses HCC migration and invasion via targeting IL6/JAK/STAT3*
327 *pathway.* Surg Oncol, 2020. **34**: p. 113-120.
328 14. Zhan, C., et al., *Development and Validation of an IL6/JAK/STAT3-Related Gene Signature to Predict*
329 *Overall Survival in Clear Cell Renal Cell Carcinoma.* Front Cell Dev Biol, 2021. **9**: p. 686907.
330 15. Siersbaek, R., et al., *IL6/STAT3 Signaling Hijacks Estrogen Receptor alpha Enhancers to Drive Breast*
331 *Cancer Metastasis.* Cancer Cell, 2020. **38**(3): p. 412-423 e9.
332 16. Wang, Q., et al., *CENPA promotes clear cell renal cell carcinoma progression and metastasis via*
333 *Wnt/beta-catenin signaling pathway.* J Transl Med, 2021. **19**(1): p. 417.
334 17. Zhang, P., et al., *ARL4C Regulates the Progression of Clear Cell Renal Cell Carcinoma by Affecting*
335 *the Wnt/beta-Catenin Signaling Pathway.* J Oncol, 2022. **2022**: p. 2724515.
336 18. Gorka, J., et al., *MCPIP1 inhibits Wnt/beta-catenin signaling pathway activity and modulates epithelial-*
337 *mesenchymal transition during clear cell renal cell carcinoma progression by targeting miRNAs.*

Oncogene, 2021. **40**(50): p. 6720-6735.
19. Xu, X., et al., *Upregulation of SDHA inhibited proliferation, migration, and invasion of clear cell renal cell carcinoma cells via inactivation of the Wnt/beta-catenin pathway.* J Recept Signal Transduct Res, 2022. **42**(2): p. 180-188.
20. Cai, J., et al., *TLN2 functions as a tumor suppressor in clear cell renal cell carcinoma via inactivation of the Wnt/beta-catenin signaling pathway.* Transl Androl Urol, 2022. **11**(1): p. 39-52.
21. Wang, L., et al., *SOX17 Antagonizes the WNT Signaling Pathway and is Epigenetically Inactivated in Clear-Cell Renal Cell Carcinoma.* Onco Targets Ther, 2021. **14**: p. 3383-3394.
22. Wang, Y., et al., *G3BP1 promotes tumor progression and metastasis through IL-6/G3BP1/STAT3 signaling axis in renal cell carcinomas.* Cell Death Dis, 2018. **9**(5): p. 501.
23. Qi, Q., et al., *Circ_0000274 contributes to renal cell carcinoma progression by regulating miR-338-3p/NUCB2 axis and JAK1/STAT3 pathway.* Transpl Immunol, 2022. **74**: p. 101626.
24. Chen, S., et al., *Tumor-associated macrophages promote migration and invasion via modulating IL-6/STAT3 signaling in renal cell carcinoma.* Int Immunopharmacol, 2022. **111**: p. 109139.
25. Song, J., et al., *The correlation between low vitamin D status and renal interleukin-6/STAT3 hyper-activation in patients with clear cell renal cell carcinoma.* Steroids, 2019. **150**: p. 108445.
26. Chae, I.G., et al., *Thymoquinone induces apoptosis of human renal carcinoma Caki-1 cells by inhibiting JAK2/STAT3 through pro-oxidant effect.* Food Chem Toxicol, 2020. **139**: p. 111253.
27. Chen, Y., et al., *SIRT1 downregulated FGB expression to inhibit RCC tumorigenesis by destabilizing STAT3.* Exp Cell Res, 2019. **382**(2): p. 111466.
28. Xiao, C., et al., *RNF7 inhibits apoptosis and sunitinib sensitivity and promotes glycolysis in renal cell carcinoma via the SOCS1/JAK/STAT3 feedback loop.* Cell Mol Biol Lett, 2022. **27**(1): p. 36.

Figure 1S Correlation of TTC13 with 8 clinicopathological characteristics including age, gender, race, grade, stage, TNM stage in ccRCC (A-H).

Figure 2S GSEA diagram of TTC13 related signaling pathways. (A) Apoptosis signaling pathway; (B) transcription factors signaling pathway; (C) JAK-STAT signaling pathway; (D) regulation of autophagy signaling pathway; (E) Renal cell carcinoma signaling pathway; (F) wnt signaling pathway.

Figure 3S The PPI network and the associations between TTC13 and MSI, TNB, TMB. (A) PPI network; (B) the association between TTC13 and MSI; (C) the association between TTC13 and TNB; (D) the association between TTC13 and TMB.

Figure 4S The associations between TTC13 and immune cell.

Figure 5S TTC13 predicts the immune response of ccRCC. (A-E) The associations between TTC13 and TAM M2, CAF, dysfunction, CD274, TIDE; (F-H) correlations between TTC13 expression and drug sensitivity. Pazopanib, Sorafenib, and Sunitinib were tested.

373 **Figure 6S** TTC13 is an independent prognostic factor of ccRCC and the establishment of nomogram. (A)
374 univariate Cox regression analysis of 8 clinicopathological parameters and TTC13 in ccRCC; (B) multivariate
375 Cox regression analysis of 8 clinicopathological parameters and TTC13 in ccRCC; (C) the nomogram for
376 predicting the survival of ccRCC patients; (D) calibration curves for 1-, 3-, and 5-year survival of ccRCC
377 patients.

Figure 1

The flow chart of this article.

The flow chart of this article.

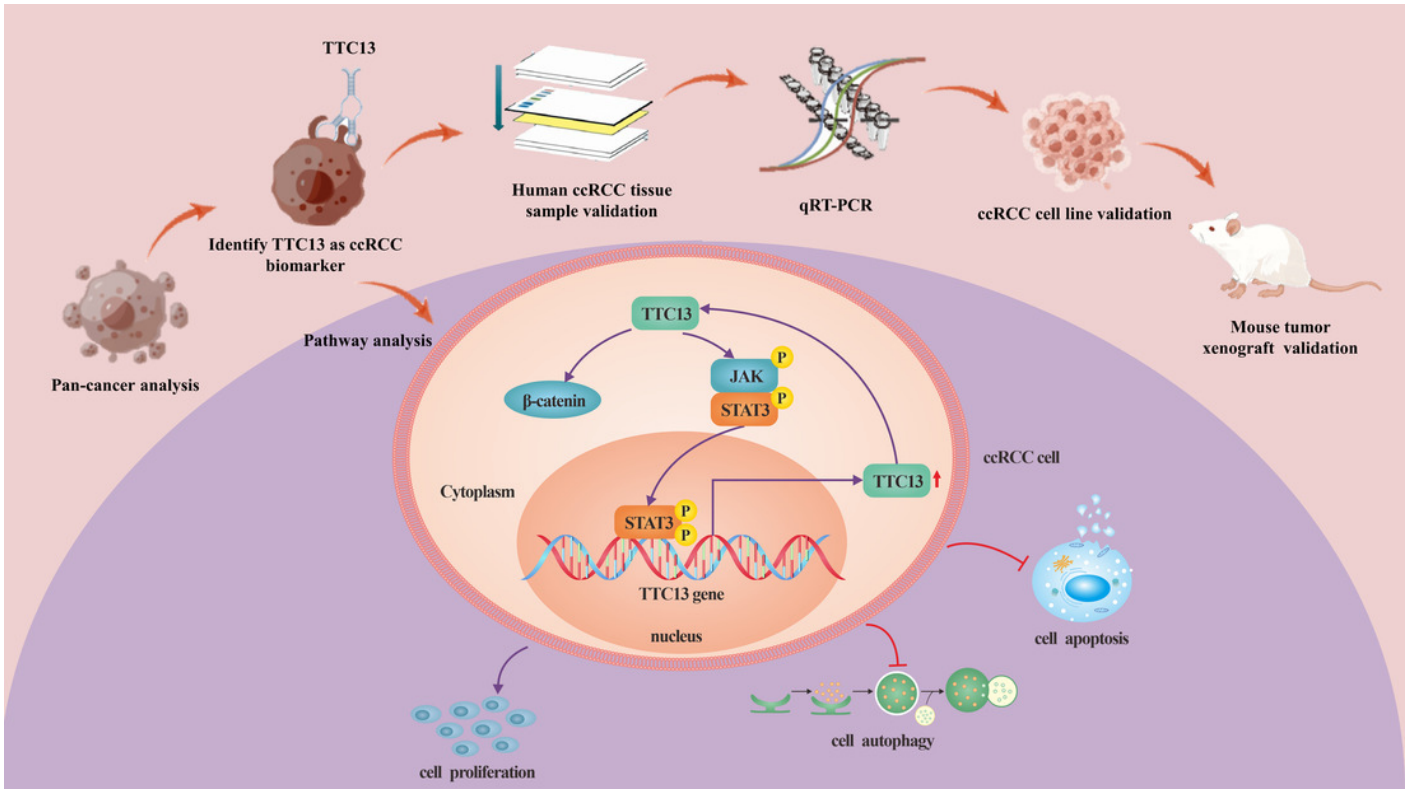

Figure 2

Expression and clinical significance of TTC13 in ccRCC.

(A) The differential expression of TTC13 in various tumors and normal samples based on the TCGA database; (B) the differential expression of TTC13 between ccRCC and normal tissues (tumor = 539, normal = 72) ($P < 0.001$); (C) pairing diagram of TTC13 expression in ccRCC and normal tissues (tumor = 72, normal = 72) ($P < 0.001$); (D) the verification of TTC13 expression in clinical samples by RT-PCR (tumor = 64, normal = 64) ($P < 0.01$); (E) the verification of TTC13 expression in clinical samples by western blotting; (F) the verification of TTC13 expression in clinical samples by IHC; (G) TTC13 expression in ccRCC cell lines detected by western blot; (H) the ROC curves of 1-, 3-, and 5-year survival of ccRCC patients; (I) K–M survival analysis of TTC13 in ccRCC ($P < 0.001$).

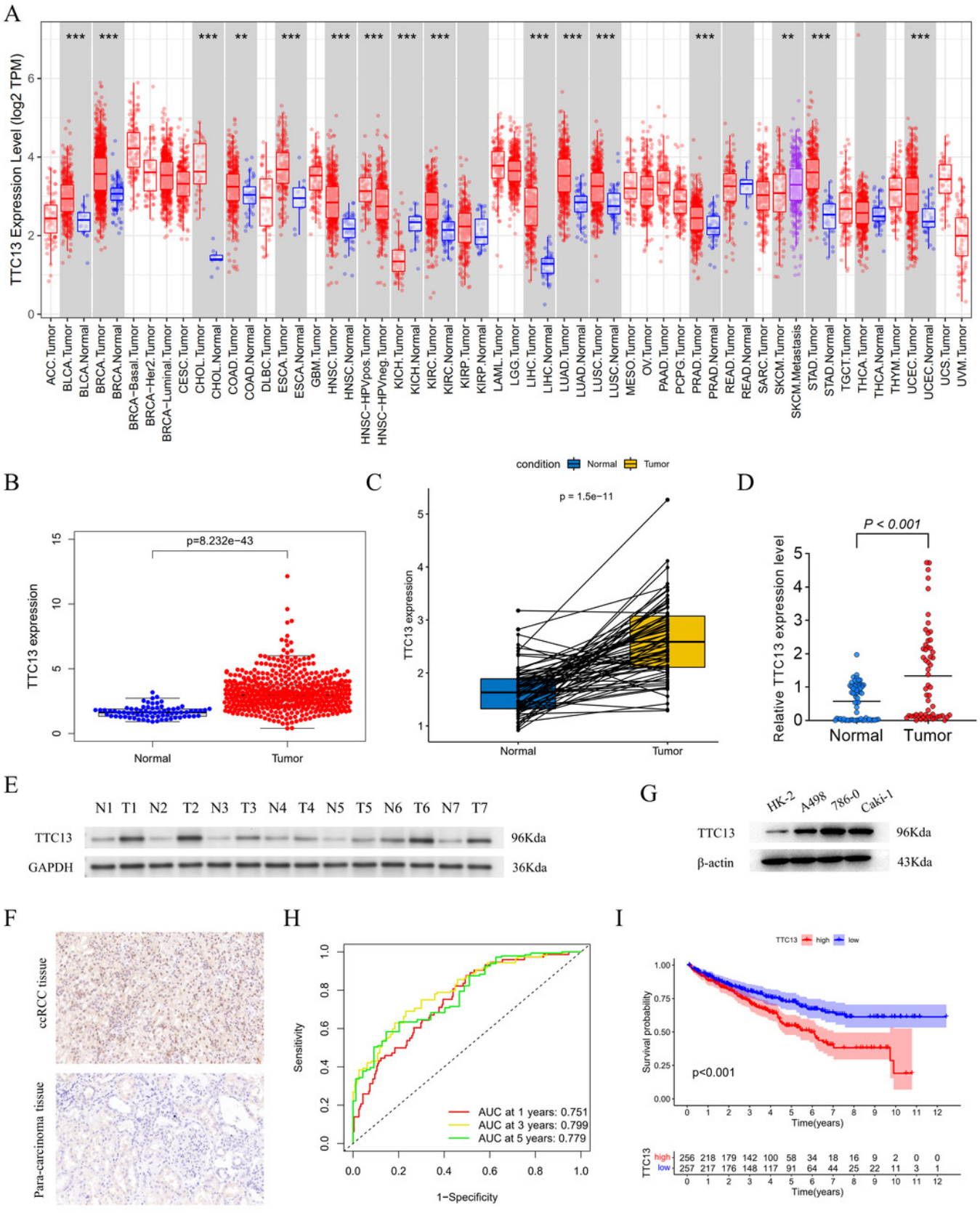
A
TTC13 Expression Level (log2 TPM)
B
p=8.232e−43
TTC13 expression
Normal
Tumor
C
condition Normal Tumor
p = 1.5e−11
TTC13 expression
Normal
Tumor
D
P < 0.001
Relative TTC13 expression level
Normal
Tumor
E
N1 T1 N2 T2 N3 T3 N4 T4 N5 T5 N6 T6 N7 T7
TTC13
GAPDH
96Kda
36Kda
G
HK-2 A498 786-0 Caki-1
TTC13
β-actin
96Kda
43Kda
F
ccRCC tissue
Para-carcinoma tissue
H
Sensitivity
1−Specificity
AUC at 1 years: 0.751
AUC at 3 years: 0.799
AUC at 5 years: 0.779
I
TTC13 high low
Survival probability
p<0.001
Time(years)
TTC13
high 256 218 179 142 100 58 34 18 16 9 2 0 0
low 257 217 176 148 117 91 64 44 25 22 11 3 1
Time(years)

Figure 3

TTC13 promoted the proliferation and inhibited the apoptosis and autophagy in ccRCC.

786-O and Caki-1 cells were transfected with pLTTC13, shTTC13 or vector controls. The proliferation of 786-O (A) and Caki-1 (B) cells was measured by CCK-8; The apoptosis and autophagy related protein expression of 786-O and Caki-1 cells was analyzed by flow cytometry(C) and western blot (D, E), respectively.

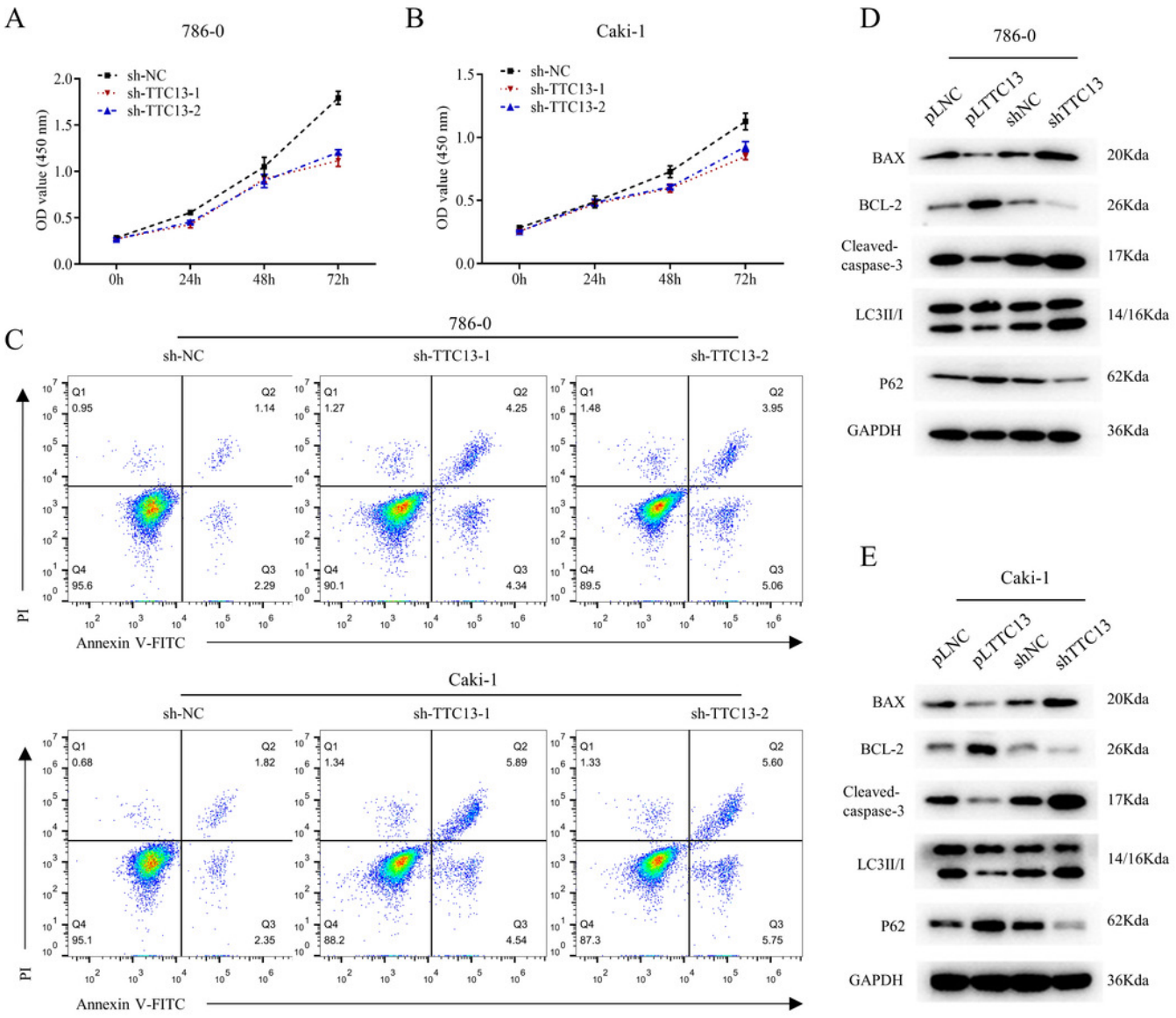

Figure 4

TTC13 silencing inhibited tumor growth in vivo.

(A) shTTC13 or vector control-transfected 786-O cells were injected subcutaneously into nude mice; (B) Tumors from mice in the two groups; (C) Comparison of tumor volumes between the two groups;(D) Comparison of tumor weight between the two groups; (E) IHC staining of the indicated tumor tissues.

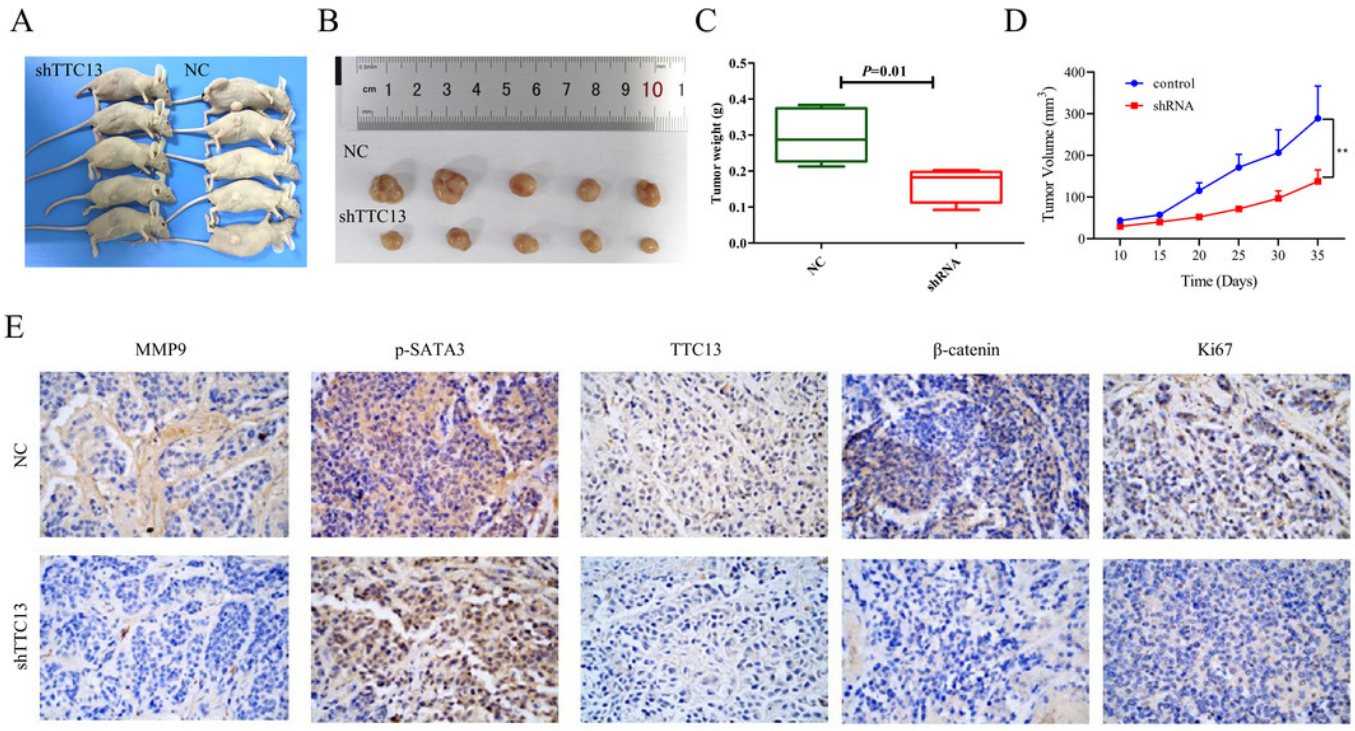

Figure 5

TTC13 related signaling pathways in ccRCC.

(A) Up- and down-regulated signaling pathways were identified by GSVA analysis; (B) the expression of wnt /β-catenin signaling pathway in 6 paired ccRCC tissues; (C) the expression of IL6-JAK-STAT3 signaling pathway in 6 paired ccRCC tissues; (D) TTC13 overexpression activated wnt/β-catenin and IL6-JAK-STAT3 signaling pathways, while knockdown of TTC13 displayed the opposite effect.

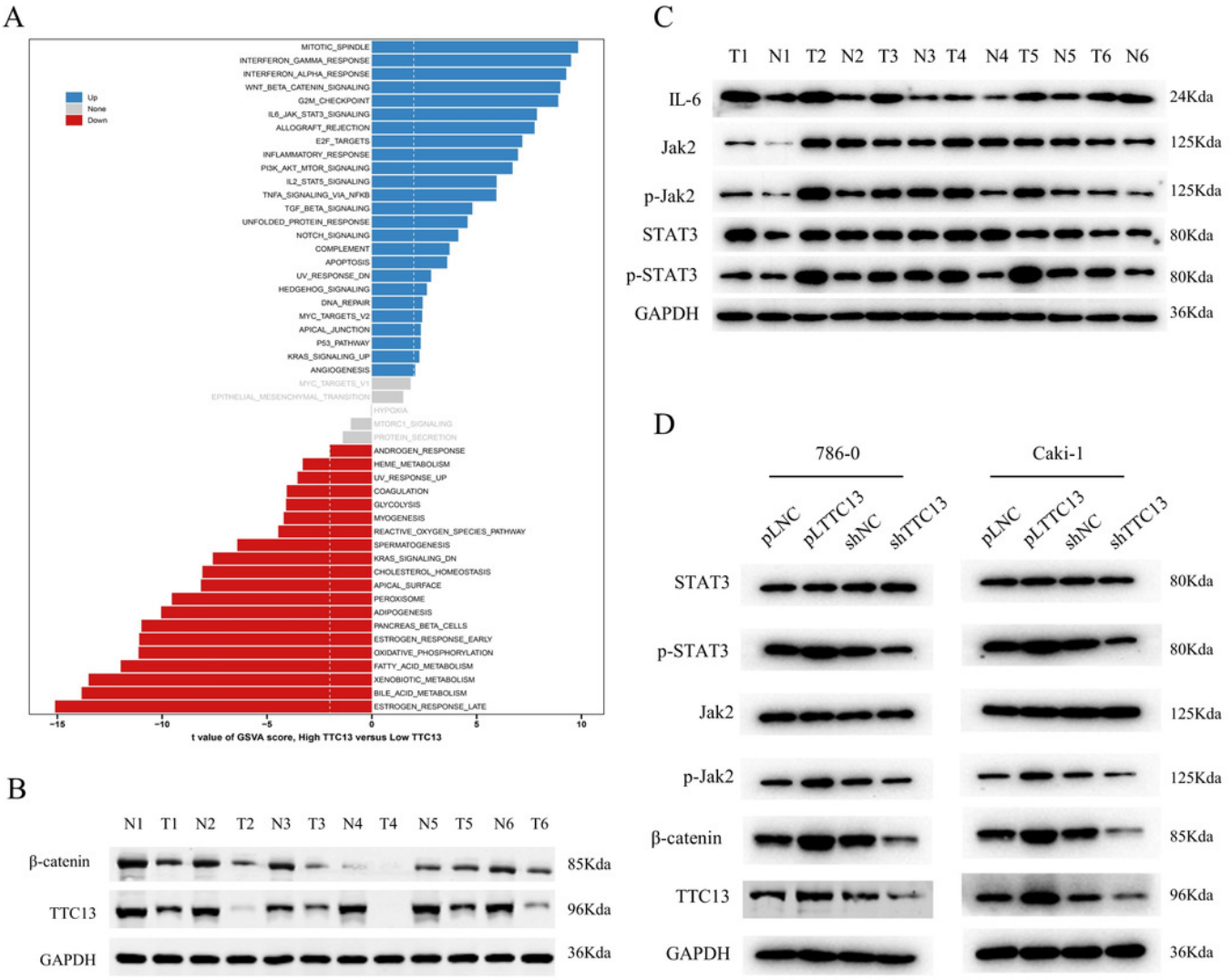

Figure 6

TTC13 promoted ccRCC growth through wnt/β-catenin and IL6-JAK-STAT3 signaling pathway.

(A) 786-O and Caki-1cell apoptosis by the flow cytometry; TTC13 promoted 786-O (B) and Caki-1(C) cell proliferation via wnt/β-catenin and IL6-JAK-STAT3 signaling pathways, as determined by CCK-8 assay; Western blot analysis of TTC13 regulated wnt/β-catenin and IL6-JAK-STAT3 signaling pathways in 786-O(D) and Caki-1(E) cells.

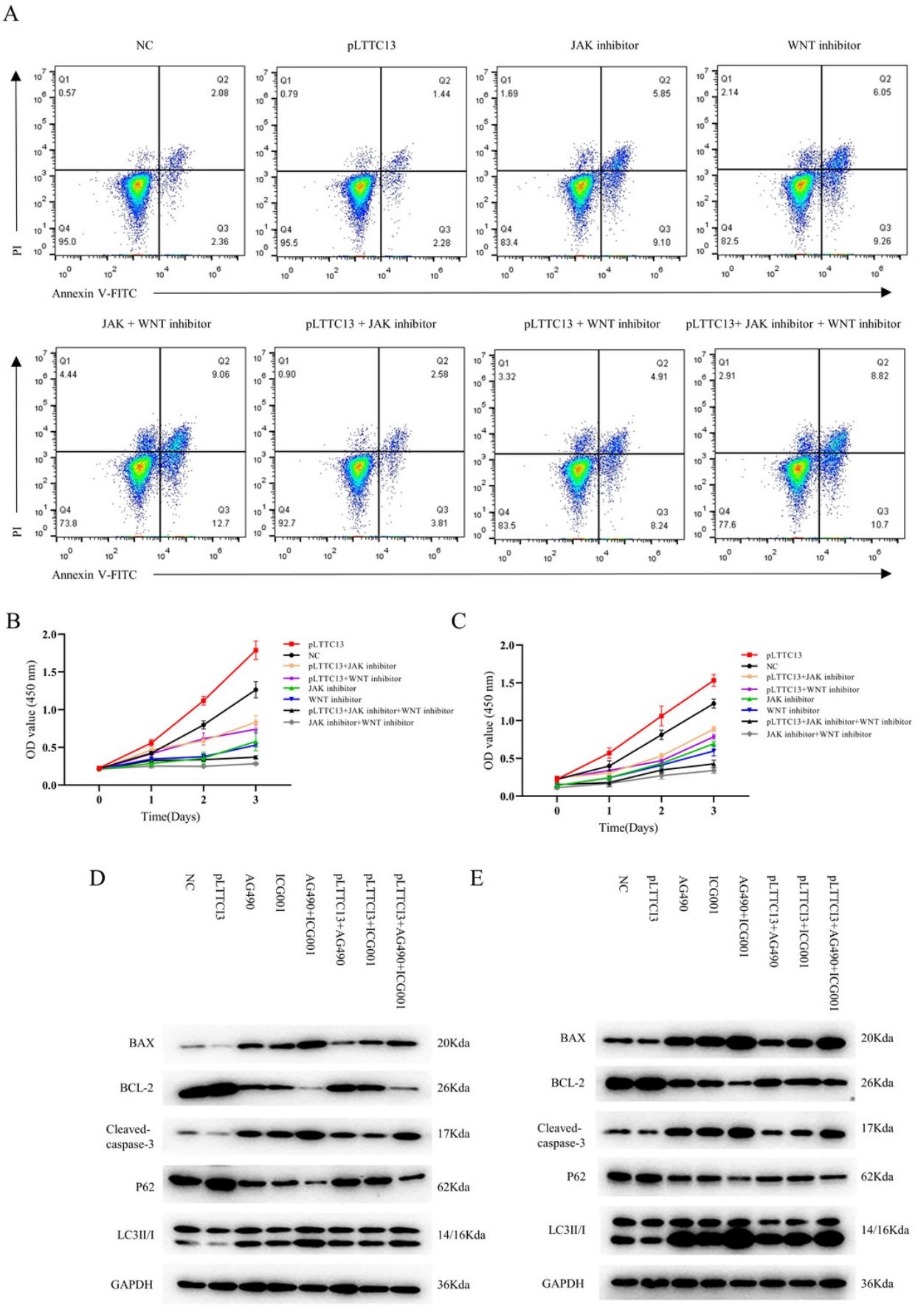
A
NC
pLTTC13
JAK inhibitor
WNT inhibitor
JAK + WNT inhibitor
pLTTC13 + JAK inhibitor
pLTTC13 + WNT inhibitor
pLTTC13+ JAK inhibitor + WNT inhibitor
PI
Annexin V-FITC
B
OD value (450 nm)
Time(Days)
pLTTC13
NC
pLTTC13+JAK inhibitor
pLTTC13+WNT inhibitor
JAK inhibitor
WNT inhibitor
pLTTC13+JAK inhibitor+WNT inhibitor
JAK inhibitor+WNT inhibitor
C
OD value (450 nm)
Time(Days)
D
E
NC
pLTTC13
AG490
ICG001
AG490+ICG001
pLTTC13+AG490
pLTTC13+ICG001
pLTTC13+AG490+ICG001
BAX
BCL-2
Cleaved-caspase-3
P62
LC3II/I
GAPDH
20Kda
26Kda
17Kda
62Kda
14/16Kda
36Kda

Figure 7

STAT3 regulated TTC13 expression at the transcription level.

(A, B) Specific binding sites of STAT3 in the promoter region of TTC13 gene; (C) Chip experiments confirmed that STAT3 directly bounded to TTC13 promoter; (D) The luciferase reporter assay confirmed the binding of STAT3 to TTC13 promoter region; (E) Immunofluorescence staining demonstrated a clear STAT3 nuclear translocation induced by TTC13 overexpression.

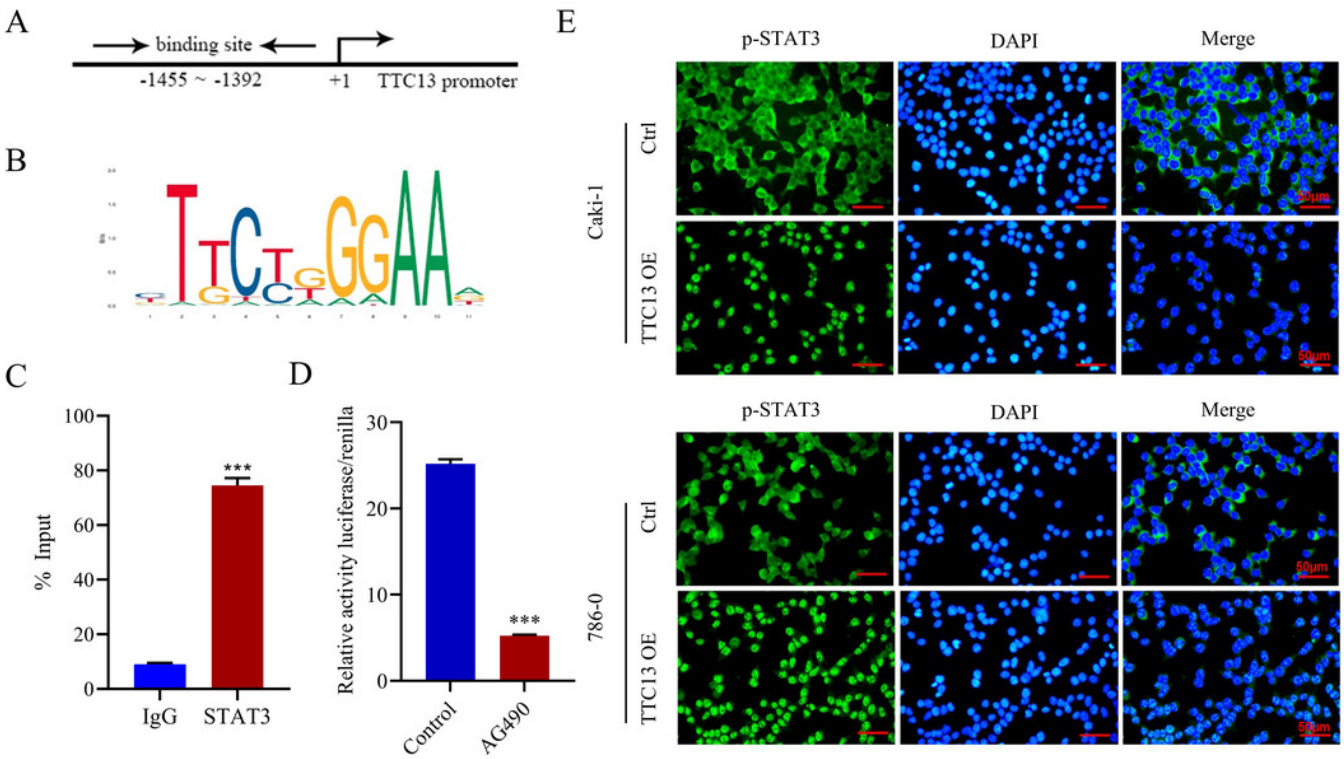

Figure 8

A working model of TTC13 regulation in ccRCC cells.

A working model of TTC13 regulation in ccRCC cells.